Materials Science Forum
ISSN: 1662-9752, Vol. 1105, pp 159-165
doi:10.4028/p-C6bEBF

Submitted: 2023-05-31
Revised: 2023-08-28
Accepted: 2023-08-28
Online: 2023-11-29

Prediction of TTR Diagrams via Physically Based Creep Simulations of Martensitic 9-12% Cr-Steels

WITZMANN Laura[1,a*], RIEDLSPERGER Florian[1,b], MERGL Josef[2,c], ZUDERSTORFER Gerold[1,d], KRENMAYR Bernhard[1,e] and SONDEREGGER Bernhard[1,f]

[1]Institute for Engineering Materials – Metals and Alloys, Johannes Kepler University Linz, Austria

[2]Institute of Numerical Mathematics, Johannes Kepler University Linz, Austria

[a]laura.witzmann@jku.at, [b]florian.riedlsperger@jku.at, [c]josef.mergl@jku.at, [d]gerold.zuderstorfer@jku.at, [e]bernhard.krenmayr@jku.at, [f]bernhard.sonderegger@jku.at

Keywords: time-to-rupture diagram, martensitic 9-12% Cr-steel, dislocation creep, modelling

Abstract. This work deals with the prediction of time-to-rupture (TTR) diagrams of martensitic 9-12% Cr steels. Martensitic 9-12% Cr steels are state of the art materials for powerplants due to their high creep strength and oxidation resistance. Since the experimental determination of TTR diagrams is costly and time-expensive (minimum 10 years), it is of particular interest to be able to model TTR diagrams and gradually replace experiments.

Here, we approach the question to what extent we can generate a TTR diagram of a material out of a fraction of experimental results plus detailed understanding of the underlying microstructural/physical phenomena during creep. Our model is based on dislocation creep and includes multiple interactions between the microstructural constituents.

We show the applicability of our approach by reproducing a TTR diagram of the well-known material P92. Input parameters are basic material data from literature, the starting microstructure before creep, chemical composition, some model parameters determined on the similar material P91, and one single creep curve of P92. The precipitate evolution is simulated by the software MatCalc, the other microstructural constituents (dislocation densities, subgrain boundaries etc.) by our creep model. By varying the stress between individual creep simulations whilst keeping all input parameters (starting microstructure, temperature and material parameters) constant, we produce multiple creep curves and thus generate the complete dataset for a TTR diagram.

The model is of particular interest when it comes to the development of new materials, as the application range of these materials can be estimated quickly and with good reproducibility.

Introduction

Components of thermal power plants have to fulfill a number of specifications, such as a high creep strength, oxidation resistance, sufficient ductility, economical manufacturing etc. [1]. Predestined materials for such requirements are martensitic 9-12% Cr-steels such as P91, P92 or FB2. This paper focuses on the material X10CrWMoVNb 9-2, better known as P92.

For the design of components such as heat exchangers or boilers, it is particularly important to extrapolate their lifetime and avoid unacceptable deformation or even failure. Since experimental methods for this task are extremely costly and time-consuming (+10 years), the prediction of creep deformation and rupture times using modelling approaches can help to better understand the results and shorten the experimental times. In this work, we use a dislocation creep model, developed by our research group.

Creep Model of the IMK (Institute of Engineering Materials – Metals and Alloys) group

In order to better predict the creep behavior of a material, a (semi-) physical dislocation creep model has been developed by our research group [2], taking the initial microstructure and precipitation data (e.g. from MatCalc) as input and generating the microstructure evolution during creep, creep curves and TTR diagrams as output. The model is based on the fundamental creep model of Ghoniem et al. [3], which was combined with the damage model of Basirat et al. [4], by Yadav [5]. Finally, the model was improved and extended by Riedlsperger et al. [2]. The model builds on interactions of mobile dislocations (density ρ_m), static dislocations (density ρ_s), boundary dislocations (density ρ_b), subgrains (radius R_{sbg}) and precipitates and deduces the time-evolution of these constituents. The current creep strain rate $\dot{\varepsilon}$ (Eq.1), which is depending on the specific microstructure in each timestep, is then calculated using Orowan's law [6], which has been slightly modified [2,7]. To consider dislocation climb over precipitates, the glide velocity v_g was replaced by an effective velocity v_{eff} [2]. In addition, the effect of cavitation damage was included [7].

$$\frac{d\varepsilon}{dt} = \frac{b \cdot \rho_m \cdot v_{eff}}{M \cdot (1 - D_{cav})} \tag{1}$$

Here, b represents the Burgers vector, M the Taylor factor and D_{cav} a parameter for cavitation damage. The current status of the creep model is described in book chapter [7] and the equations are explained in detail in reference [2]. It should be noted that the damage models are different in these two references. In this work, the damage law was further improved (see Eq. 2), so that the tertiary region of the creep curve is simulated more realistically. In this equation, A represents a specific phenomenological material parameter for the tertiary region.

$$\dot{D}_{cav} = A \cdot \varepsilon \cdot \dot{\varepsilon}^{\,0.8} \tag{2}$$

The IMK dislocation creep model was developed with the benchmark material P91 and has so far been successfully applied to 5 different materials, including P92 [8]. In Riedlsperger et al. [8], an older version of our model was used (2022). The main difference between the previous publication and the present work is an updated damage model. Precipitate damage (as suggested by [4,5]) was excluded from Orowan's law, since it is already implicitly included by coarsening of precipitates. Moreover, the exponent of the strain rate in the cavitation damage law was optimized from 1 [2,5] and 0.5 [7] to 0.8 in this work to obtain a better depiction of the tertiary creep area with decreasing stresses. Furthermore, the precipitate simulations have been improved (mod. Z-phase nucleates after several thousand hours in contrast to the reference [8]). In Riedlsperger et al. [8], only TTR data for 650°C and 600°C were calculated. In this work, TTR data for 625°C were additionally simulated. Moreover, we complemented our calculated TTR data at 650°C by modelled times-to-1%-strain (TT1%). Finally, a better agreement to experimental creep curves has been achieved by introducing an optimization algorithm [9].

Model Setup: Precipitation Kinetic Simulation with MatCalc

A thermodynamic precipitation kinetic simulation was carried out with the software MatCalc [10] (based on the SFFK theory [11]) for modelling the precipitate evolution, considering nucleation, growth and coarsening events. The results (radius r_i and number density $N_{v,i}$) were then imported into the creep equation framework to combine the two simulations. The composition used for P92 is shown in Table 1, adopted from Riedlsperger et al. [8] (except B) according to ASTM A335 [12].

Table 1. P92 composition for the precipitation kinetic simulations in MatCalc [wt.%]

Fe	Al	C	Cr	Mn	Mo	N	Nb	Ni	Si	V	W	B
bal.	0.01	0.10	9.0	0.45	0.45	0.05	0.064	0.35	0.35	0.20	1.75	0.0035

The virtual heat treatment consisted of normalising at 1050°C for 30 min and tempering at 765°C for 1 h [8]. $M_{23}C_6$, Laves-phase, MX carbo-nitrides (split into VN and NbC), AlN and the modified Z-phase CrVN were considered in the simulation. According to a previous Scheil calculation in MatCalc, no primary phases are present. Furthermore, the selected nucleation sites were subgrain boundaries (for NbC, VN, $M_{23}C_6$, Laves phase), dislocations (NbC, VN, Al), and VN for the mod. Z-phase, to account for on-particle nucleation [13]. The mobile dislocation evolution during the heat treatment was calculated using the static recovery part (see [13] for the procedure) of a state-parameter-based ABC-model [14], based on the experimental investigations of [15].

Subsequently, the precipitate evolution simulation was carried out at the three exposure temperatures; 650°C, 625°C and 600°C, respectively, taking the final precipitate status after the heat treatment simulation as starting point. Fig. 1 shows the result for 650°C, depicting the volume-weighted diameter and the number densities (nucleation at mart=martensitic matrix, aust=austenitic matrix, g=grain boundaries, d=dislocations, s=subgrain boundaries, VN_m_d/VN_m_s=on-particle nucleation at VN(mart,d)/VN(mart,s)). Phases represented by solid lines are included in the creep equation framework, phases shown by dashed lines are neglected, due to their low phase fraction (AlN) or quick dissolution (NbC(mart,d)). The effect of modified Z-phase is considered indirectly by the phase fraction drop of VN(mart,s) during the transformation process. After finishing the precipitate simulation, the precipitate coarsening is quantified by the Ostwald ripening parameter k_p for loading the MatCalc results into the creep simulation (Table 2).

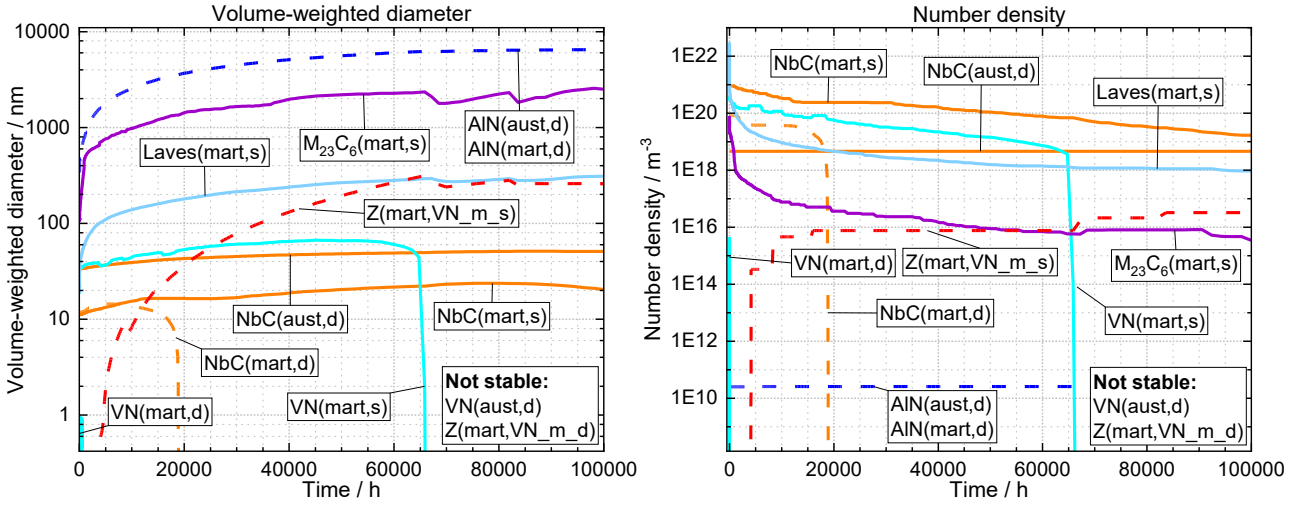

Fig. 1. Simulated volume-weighted diameter (left) and number density (right) of P92 with MatCalc for 650°C ageing

Table 2. Ostwald-ripening parameters deduced from MatCalc simulations of 100.000h; <0.006 % phase fraction not stated;

Precipitate	Ostwald-ripening parameter k_p [s^{-1}]			Precipitate	Ostwald ripening parameter k_p [s^{-1}]		
	650°C	625°C	600°C		650°C	625°C	600°C
$M_{23}C_6$(mart,s)	$1.5\cdot10^{-4}$	$4.8\cdot10^{-6}$	$1.9\cdot10^{-6}$	**Laves(mart,s)**	$1.4\cdot10^{-3}$	$5.1\cdot10^{-4}$	$9.8\cdot10^{-5}$
VN(mart,s)*	$1.8\cdot10^{-7}$	$1.5\cdot10^{-7}$	$1.4\cdot10^{-7}$	**NbC(mart,s)**	$1.2\cdot10^{-8}$	$5.4\cdot10^{-9}$	$3.3\cdot10^{-9}$
NbC(aust,d)	$8.5\cdot10^{-9}$	$5.1\cdot10^{-9}$	$1.9\cdot10^{-9}$	**NbC(mart,d)***	-	$-1.3\cdot10^{-9}$	$2.4\cdot10^{-9}$

*It should be noted, that VN(mart,s) and NbC(mart,d) in Table 2 are only considered until they dissolve (excluding NbC(mart,d) at 650°C, as it already dissolves after < 20.000 h).

Creep model setup: Microstructural parameters

To calculate a master creep curve for a given temperature and stress, further input parameters are required in addition to the precipitate evolution from MatCalc. These parameters include: (i) the initial microstructure of the material (determined by experiments or taken from the literature), (ii) 16 basic

physical parameters (e.g. Young's Modulus), (iii) two fundamental constants (taken from the literature) (iv) and four adaptive parameters (three of them are physical). The latter can be extracted from one single creep experiment of medium duration.

In this work, the required initial microstructural values and the physical parameters/ constants have been taken from [8]. Regarding the new equation for the tertiary region, the phenomenological parameter A has to be adjusted to A=11.6. Furthermore, a_1 is changed to 7.2 m/s, as this is a more sufficient value. The Holt constant K_c for subgrain nucleation and the source density for mobile dislocations β remain the same as in Riedlsperger et al. [8].

For the extrapolation from the master creep curve from 650°C to 625°C and 600°C, we apply a lower coarsening rate of the precipitates (Table 2), as well as lower diffusion coefficients (lattice diffusion coefficient D_s & pipe diffusion coefficient D_{vp}). Since the relaxation behavior also depends on temperature, we adapted the activation volume V_r as well. These changes are summarized in Table 3, with the activation volume V_r being expressed as a multiple of the atomic volume Ω.

Table 3. Parameter changes for creep simulations at 650°C, 625°C and 600°C

Parameter	Value			Unit	Source
	650°C	625°C	600°C		
V_r	22.35·Ω	21·Ω	13.85·Ω	[m^3]	-
D_s	$2\cdot10^{-19}$	$1.1\cdot10^{-19}$	$2\cdot10^{-20}$	[m^2/s]	[17]
D_{vp}	$4.75\cdot10^{-19}$	$2.61\cdot10^{-19}$	$4.75\cdot10^{-20}$	[m^2/s]	[2] for 650°C; (625°C/600°C: proportional to D_s)

Results: Simulated creep curve

The master creep curve is simulated for P92 at 650°C/ 118 MPa, as shown in Fig. 2 (left). The experimental curve [15] is for the same conditions. For an isothermal extrapolation to other stresses, the parameter-set from the master creep curve remains the same, only the stress is varied. The results of calculated creep curves from 60 MPa to 160 MPa can be seen in Fig. 2 (right).

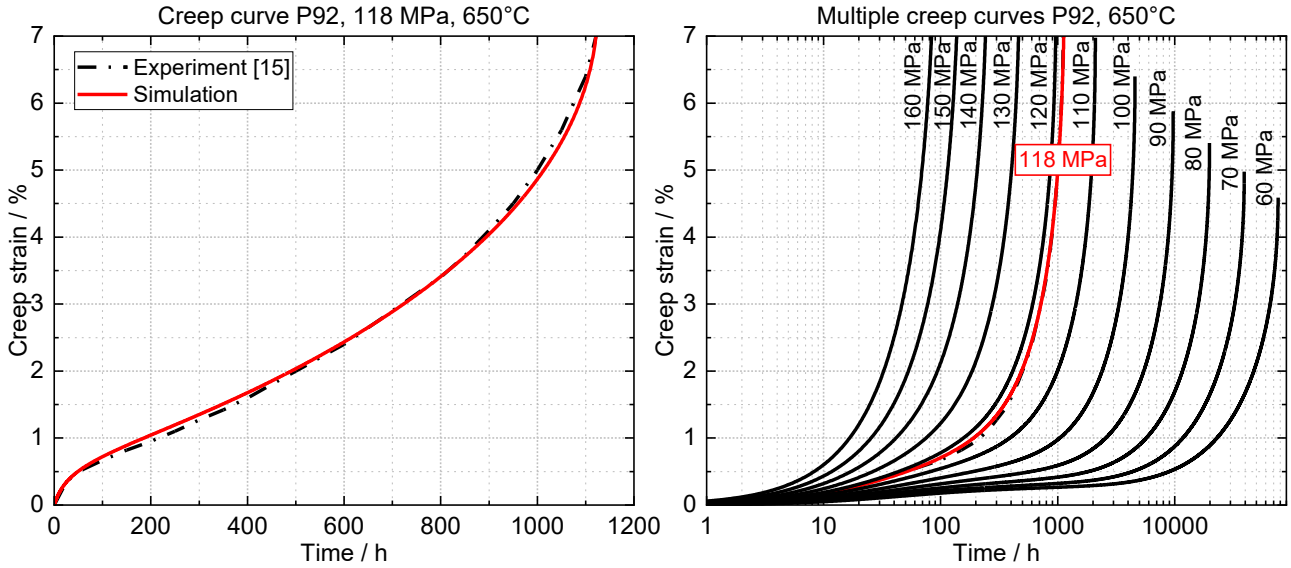

Fig. 2. Simulated and experimental (data extracted from [15]) creep curve for P92 at 650°C and 118 MPa (left); Multiple creep curves for P92 at 650°C (right)

Results: Diagram of rupture times & times to 1 % strain

By taking the rupture times from all simulated creep curves from the same temperature, we construct a TTR diagram. We carried out this procedure for the 3 temperatures 600°C, 625°C and 650°C, as shown in Fig. 3. The times-to-1%-strain (TT1%) were extracted from the simulated creep curves at 650°C. The simulated rupture times are compared to the ECCC reference for P92 from 2019 [18] and TT1% data at 650°C were compared to several experimental data extracted from the literature [15, 19-24]. It should be noted, that the experimental data point [24] is not at 650°C, but at 640°C.

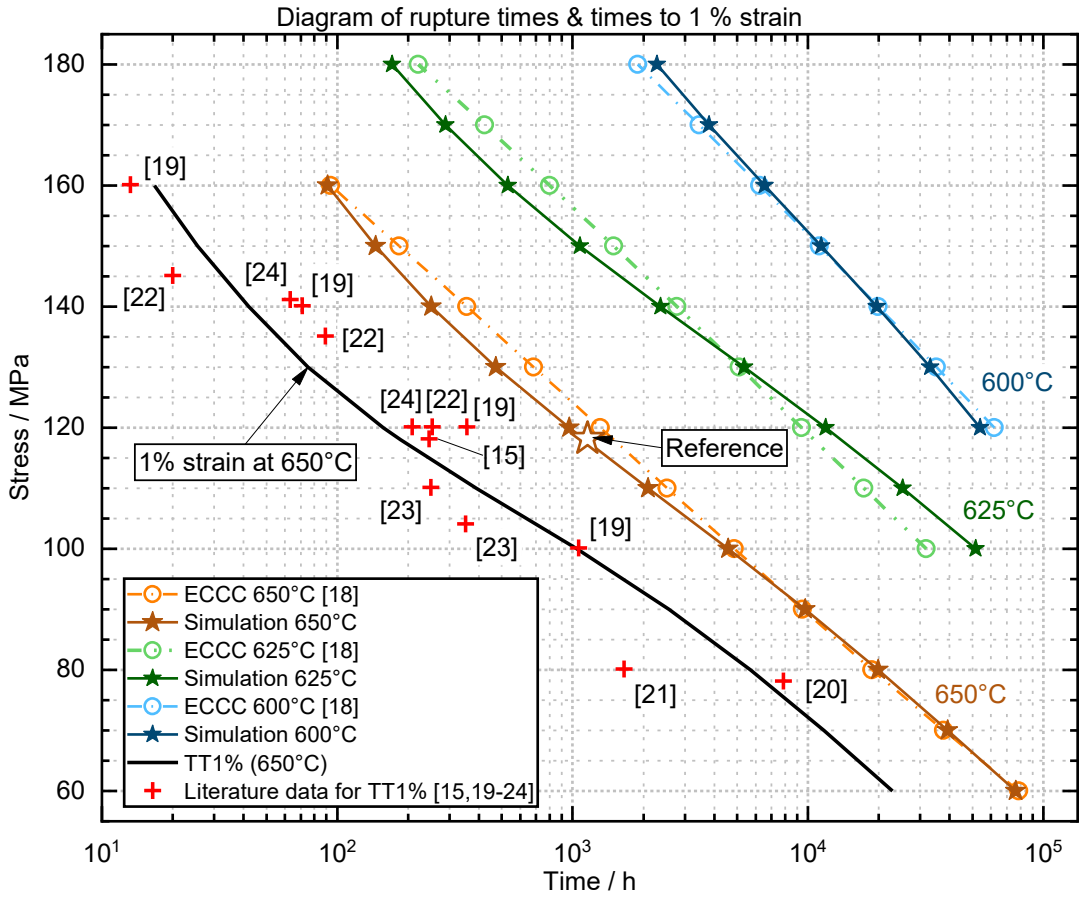

Fig. 3. Simulated time-to-rupture diagram for P92 at 600°C, 625°C and 650°C with a comparison to ECCC reference [18]; TT1% for 650°C with experimental points (extracted from [15,19-24]); [24] is at 640°C

Summary and Discussion

The creep model of our working group [2] for the material P92 has been refined, in particular by more realistic MatCalc calculations with respect to the modified Z-phase (nucleation after several thousand hours), and also by a better description of the tertiary region of the creep curves. Based on experimental data from one single creep test (650°C, 118 MPa) and some literature data, we succeeded in reproducing this reference experimental creep curve very accurately by a simulation. From this single starting point, we were able to deduce a TTR diagram for 3 different temperatures, each. Our model is capable of predicting rupture times up to 100 000 hours with excellent accuracy, when compared to ECCC reference data [18]. Our deviation with respect to stress is never larger than 6%, remaining significantly below the usual threshold of 20% for scatter bands with respect to stress. In addition, for the first time, 625°C have been simulated in the TTR diagram for P92. Moreover, we demonstrated that TT1% data for 650°C can be easily extracted from the corresponding creep curves at multiple stresses, showing very good agreement to experimental data from literature and underlining the correctness of our simulation.

In the future, we plan to extend the model to other materials-groups (such as Ni-based alloys, e.g. [25]). Our creep software CreeSo [26] will implement the current status of the IMK model, and is planned to be released soon.

Acknowledgments

This research was funded in whole, or in part, by the Austrian Science Fund (FWF) [P-31374]. For the purpose of open access, the author has applied a CC BY public copyright licence to any Author Accepted Manuscript version arising from this submission. Furthermore, L.W. would like to thank the Linz Institute of Technology (LIT), the province of Upper Austria and the Federal Ministry of Austria - Education, Science and Research (BMBWF) for financial support within the project LIT-2021-10-SEED-115,01/899978 "MLSC - Model Development for Lifetime Assessment of Steels under Various Creep Loads". J.M. gratefully acknowledge student funding from Johannes Kepler University (JKU) Linz. Financial support from Siemens Energy Global GmbH & Co. KG is gratefully acknowledged. The authors want to thank Dr. Torsten Neddemeyer & Dr. Torsten-Ulf Kern from Siemens Energy Global GmbH & Co.KG and Prof. Dr. John Hald from DTU (Technical University of Denmark) for fruitful discussions.

References

[1] J. Hald, Microstructure and long-term creep properties of 9–12% Cr steels, Int J Pres Ves Pip 85 (2008) 30-37.

[2] F. Riedlsperger, B. Krenmayr, G. Zuderstorfer, B. Fercher, B. Niederl, J. Schmid, B. Sonderegger, Application of an advanced mean-field dislocation creep model to P91 for calculation of creep curves and time-to-rupture diagrams, Materialia 12 (2020) 100760.

[3] N.M. Ghoniem, J.R. Matthews, R.J. Amodeo, A Dislocation Model for Creep in Engineering Materials, Res Mech 29 (1990) 197–219.

[4] M. Basirat, T. Shrestha, G.P. Potirniche, I. Charit, K. Rink, A study of the creep behavior of modified 9Cr-1Mo steel using continuum-damage modeling, Int J Plast 37 (2012) 95–107.

[5] S.D. Yadav, Creep study of 9-12% Cr steels for power plants, PhD Thesis, Graz University of Technology, Austria, 2016.

[6] E. Orowan, Problems of plastic gliding, P Phys Soc 52 (1940) 8–22.

[7] C. Sommitsch, B. Sonderegger, M. Ahmadi, F. Riedlsperger, F. Meixner, J. Mergl, B. Krenmayr, Microstructurally Based Modeling of Creep Deformation and Damage in Martensitic Steels, in: Abdallah Z., Aldoumani N. (Eds.), Creep Deformation, IntechOpen, London, 2022.

[8] F. Riedlsperger, G. Zuderstorfer, B. Krenmayr, B. Sonderegger, Application of a physically-based dislocation creep model to P92 for constructing TTR diagrams, Mater High Temp 39 (2022) 161–166.

[9] J. Mergl, Numerical simulation and optimization of microstructure-based creep models, Diploma Thesis, Johannes Kepler University Linz, Austria, 2022.

[10] E. Kozeschnik, Mean-Field Microstructure Kinetics Modeling, in: F.G. Caballero (Ed.), Encyclopedia of Materials: Metals and Alloys, 4, Elsevier Inc,, 2022, pp. 521-526.

[11] J. Svoboda, F.D. Fischer, P. Fratzl, E. Kozeschnik, Modelling of kinetics in multi-component multi-phase systems with spherical precipitates I: Theory, Mat Sci Eng A-Struct 385 (2004) 166–174.

[12] L. Maddi, G.S. Deshmukh, A.R. Ballal, D.R. Peshwe, R.K. Paretkar, K. Laha, M.D. Mathew, Effect of Laves phase on the creep rupture properties of P92 steel, Mat Sci Eng A 668 (2016) 215–223.

[13] F. Riedlsperger, B. Gsellmann, E. Povoden-Karadeniz, O. Tassa, S. Matera, M. Dománková, F. Kauffmann, E. Kozeschnik, B. Sonderegger, Thermodynamic modelling and microstructural study of Z-phase formation in a Ta-alloyed martensitic steel, MDPI Materials 14 (2021) 1332.

[14] S. Zamberger, L. Whitmore, S. Krisam, T. Wojcik, E. Kozeschnik, Experimental and computational study of cementite precipitation in tempered martensite, Model Simul Mater Sci Eng. 23 (2015) 055012.

[15] V. Dudko, A. Belyakov, D. Molodov, R. Kaibyshev, Microstructure Evolution and Pinning of Boundaries by Precipitates in a 9 pct Cr Heat Resistant Steel During Creep, Metall Mater Trans A. 44 (2013) 162–172.

[16] F. Riedlsperger, Microstructurally based creep modelling of selected martensitic Cr-steels and Ni-based alloys, PhD Thesis, Graz University of Technology, Austria, 2022.

[17] H. Nitta, K. Miura, Y. Iijima, Self-diffusion in iron-based Fe–Mo alloys, Acta Mater. 54 (2006) 2833–2847.

[18] ECCC Datasheet 2019 for P92.

[19] H. Kang, J. Shen, S. Zhang, H. Han, F. Hu, B. He, Q. Zhao, G. Xiao, Influence of thermal ageing on creep rupture mechanism and creep life of P92 ferritic steel, Mater Res Express. 7 (2020) 086517.

[20] M. Yoshizawa, M. Igarashi, K. Moriguchi, A. Iseda, H.G. Armaki, K. Maruyama, Effect of precipitates on long-term creep deformation properties of P92 and P122 type advanced ferritic steels for USC power plants, Mat Sci Eng A 510–511 (2009) 162–168.

[21] A. Fedoseeva, I. Nikitin, N. Dudova, R. Kaibyshev, Structural Evolution of P92-Type Martensitic Steel during Creep at 650°, Acta Phys Pol A. 134 (2018) 644–648.

[22] Y. Chang, H. Xu, Y. Ni, X. Lan, H. Li, The effect of multiaxial stress state on creep behavior and fracture mechanism of P92 steel, Mat Sci Eng A. 636 (2015) 70–76.

[23] S.D. Yadav, B. Sonderegger, M. Stracey, C. Poletti, Modelling the creep behaviour of tempered martensitic steel based on a hybrid approach, Mat Sci Eng A. 662 (2016) 330–341.

[24] N.Q. Zhang, H. Xu, X.P. Mao, G. Wang, Study on High Temperature Creep Behaviors of P92 Steel, Key Eng Mater. 452–453 (2010) 521–524.

[25] F. Riedlsperger, T. Wojcik, R. Buzolin, G. Zuderstorfer, M. Speicher, C. Sommitsch, B. Sonderegger, Microstructural insights into creep of Ni-based Alloy 617 at 700°C provided by electron microscopy and modelling, Mater. Charact. 198 (2023) 112720.

[26] G. Zuderstorfer, F. Riedlsperger, B. Sonderegger, CreeSo – software for creep simulation of complex alloys, Mater High Temp 39 (2022) 596–602.